

of the crystallographic positions were generally smaller than and in poor agreement with the crystallographic values.¹⁵

We find that the behavior of the hydrate in β - and γ -cyclodextrin is completely analogous to that observed in more complicated crystalline proteins such as crambin, lysozyme, and ribonuclease^{3,6} in terms of the low degree of hydrate order, the temperature dependence of the ordering, and translational diffusion in the lattice, from the perspective of the deuterium NMR experiment. The observations here potentially resolve the apparent disagreement between the deuterium NMR studies and diffraction studies of crambin. The NMR studies indicate a highly mobile and disordered hydrate whereas the X-ray structure was refined to include well-defined hydrate networks.¹⁹

Finally we note that, in correspondence with the low degree of ordering observed for the hydrate, included ethanol or benzyl alcohol are also orientationally disordered within the β -CD cavity to a substantial degree. The residual deuterium quadrupole coupling, qcc, and asymmetry, η , calculated from the X-ray structures are larger than the values measured by NMR spectroscopy, showing that the X-ray structures overestimated the

orientational ordering of the molecule included in the cavity. Furthermore, inclusion of NMR visible and X-ray diffraction invisible processes such as methyl group rotations, 180° ring flips, or planar ring rotations does not resolve the discrepancies. Thus, a single hydrogen bonding group and packing constraints do not severely limit the allowed orientations of these molecules stoichiometrically included in the cavity. This is an interesting result in light of the known catalytic properties of cyclodextrins which in part arise from their ability to orient substrates relative to catalytic groups in analogy to enzymes.

Note Added in Proof. A recent quasielastic incoherent neutron scattering study of β -CD·11D₂O by Steiner et al. (*Mol. Phys.* **1991**, *72*, 1211-1232) with higher energy resolution than previously reported¹⁴ shows diffusive motions of the water molecules at room temperature in β -CD·11D₂O in agreement with the results presented here.

Acknowledgment. We wish to thank Professor John Richardson for his expert guidance with the x-ray measurements and Professor Hugh Savage for suggesting to us the cyclodextrin system. This work was supported by a biophysics grant from the National Science Foundation (DMB8918376).

(19) Teeter, M. M. *Proc. Natl. Acad. Sci. U.S.A.* **1984**, *81*, 6014-6018.

NMR Studies of Iron(II) Nitrosyl π -Cation Radicals of Octaethylchlorin and Octaethylisobacteriochlorin as Models for Reaction Intermediate of Nitrite Reductase

Shinji Ozawa, Hiroshi Fujii,[†] and Isao Morishima*

Contribution from the Division of Molecular Engineering, Graduate School of Engineering, Kyoto University, Kyoto 606, Japan. Received May 17, 1991

Abstract: Chemical oxidation of iron(II) nitrosyl complexes of octaethylchlorin (OEC) and octaethylisobacteriochlorin (OEiBC) yielded iron(II) nitrosyl π -cation radicals. The π -cation radicals afforded well-resolved hyperfine-shifted NMR resonances characteristic of an a₂ π -radical state. Non-Curie law behavior of the deuterium NMR resonances was interpreted in terms of a valence isomerization from the chlorin π -cation radical to the Fe^{II}NO⁺ chlorin complex due to ligation of SbF₆⁻ to the iron of the π -cation radical as well as a magnetic interaction between the NO and π -radical spins in (OEiBC)Fe^{II}NO π -cation radical. This valence isomerization was confirmed by variable-temperature electronic absorption spectral measurements. Furthermore, ligation of imidazole to the π -cation radicals caused valence isomerization to yield (OEC)Fe^{II}(NO⁺)(Im) and (OEiBC)Fe^{II}(NO⁺)(Im) complexes.

Introduction

Heme-like prosthetic groups derived from dihydroporphyrins exist in a variety of redox enzymes. The presence of a *d*-type cytochrome in several microorganisms was discovered many years ago, and the green prosthetic group has been found to be an iron chlorin (dihydroporphyrin).¹ Recently, nitrite reductase has also been shown to contain iron hydroporphyrins (iron chlorin and iron isobacteriochlorin) as the prosthetic group.²⁻⁵ The enzyme catalyzes the multielectron reduction of nitrite to ammonia or to nitric oxide. Dissimilatory nitrite reductase having heme *d*₁ as a prosthetic group catalyzes reduction of nitrite to nitric oxide.³ Assimilatory nitrite reductase, possessing an iron isobacteriochlorin referred to as siroheme, catalyzes six-electron reduction of nitrite to ammonia.² A nitrite reductase which contains iron chlorin has also been isolated from *Aspergillus niger*.⁵ Although the whole reduction mechanism (from **1** to **3**) for these nitrite reductases

has not yet been established, an iron(II) nitrosyl complex (**2**) has been detected⁶⁻⁸ as a reaction intermediate in the reduction cycles of nitrite to nitric oxide or to ammonia, as described below.

(1) (a) Keilin, D. *Nature* **1933**, *64*, 783. (b) Barrett, J. *Biochem. J.* **1956**, *132*, 626-639.

(2) (a) Siegel, L. M.; Murphy, M. J.; Kamin, H. *J. Biol. Chem.* **1973**, *248*, 251-264. (b) Murphy, M. J.; Siegel, L. M.; Kamin, H. *Ibid.* **1973**, *248*, 2801-2804. (c) Murphy, M. J.; Siegel, L. M.; Tove, S. R.; Kamin, H. *Proc. Natl. Acad. Sci. U.S.A.* **1974**, *250*, 7980-7989.

(3) Kim, C. H.; Hollocher, T. C. *J. Biol. Chem.* **1983**, *258*, 4861-4863.

(4) (a) Kuronen, T.; Ellfolk, N. *Biochim. Biophys. Acta.* **1972**, *275*, 308-318. (b) Newton, N. *Biochim. Biophys. Acta* **1969**, *185*, 316-331. (c) Le Gall, J.; Payne, W. J.; Morgan, T. V.; DerVartanian, D. V. *Biochem. Biophys. Res. Commun.* **1979**, *87*, 355-362. (d) Iwasaki, H.; Matsubara, T. *J. Biochem.* **1971**, *69*, 847-857. (e) Cox, C. D.; Payne, W. J.; DerVartanian, D. V. *Biochim. Biophys. Acta* **1971**, *253*, 290-294.

(5) Horie, S.; Watanabe, T.; Nakamura, S. *J. Biochem.* **1976**, *80*, 579-593.

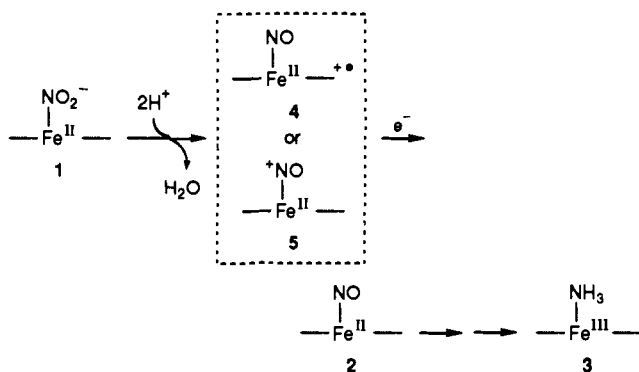
(6) Johnson, M. K.; Thomson, A. J.; Walsh, T. A.; Barber, D.; Greenwood, C. *Biochem. J.* **1980**, *189*, 285-294.

(7) Lancaster, J. R.; Vega, J. M.; Kamin, H.; Orme-Johnson, N. R.; Orme-Johnson, W. H.; Krueger, R. J.; Siegel, L. M. *J. Biol. Chem.* **1979**, *254*, 1268-1272.

(8) Apario, P. J.; Knaff, D. B.; Malkin, R. *Arch. Biochem. Biophys.* **1975**, *169*, 102-107.

* To whom correspondence should be addressed.

[†] Present address: The Department of Chemistry, Faculty of Science, Hokkaido University, Sapporo 060, Japan.



In the reduction reaction from 1 to 2, there could be two possible reduction pathways which go through putative intermediates, either the $\text{Fe}^{\text{II}}\text{NO}$ π -cation radical (4) or $\text{Fe}^{\text{II}}\text{NO}^+$ (5) (or $\text{Fe}^{\text{III}}\text{NO}$ (6)) complex.^{3,9-12,13b} It is therefore of interest to determine and characterize the intermediates (4 and 5) by using model complexes of iron chlorin and iron isobacteriochlorin. Since the model nitrite complex (1) is not stable^{14,15} enough for examining reduction products, formation of the nitrosyl intermediate (4 or 5) could be facilitated by oxidation of the stable complex 2. Along with this line, Fujita and Fajer¹¹ studied the electrochemical oxidation of iron(II) nitrosyl octaethylchlorin and isobacteriochlorin, (OEC) $\text{Fe}^{\text{II}}\text{NO}$ and (OEiBC) $\text{Fe}^{\text{II}}\text{NO}$,¹⁶ and suggested the formation of the π -cation radicals rather than the $\text{Fe}^{\text{III}}\text{NO}$ (or $\text{Fe}^{\text{II}}\text{NO}^+$) complexes. On the contrary, oxidation of the corresponding octaethylporphyrin (OEP) complex gave rise to the $\text{Fe}^{\text{III}}\text{NO}$ complex.¹¹ These π -cation radicals were ESR silent possibly due to enhanced electron spin relaxation caused by NO spin- π radical spin interaction, and therefore their electronic structures have remained open to further studies. The effect of the axial ligand on the oxidation site of $\text{Fe}^{\text{II}}\text{NO}$ complexes has not yet been studied. This ligand effect could have some biological significance, because in nitrite reductase heme d_1 is coordinated by the nitrogenous ligand, possibly histidyl imidazole.⁶

We have studied the electronic structures of one-electron chemical oxidation products of (OEC) $\text{Fe}^{\text{II}}\text{NO}$ and (OEiBC)- $\text{Fe}^{\text{II}}\text{NO}$ and their ligation effects. It is shown here that oxidized products afford well-resolved hyperfine-shifted NMR resonances characteristic of chlorin and isobacteriochlorin π -cation radicals, from which the type of radical orbital (a_2 or b_2) is readily determined. It is also demonstrated that the axial ligation converts the π -cation radical to an $\text{Fe}^{\text{II}}\text{NO}^+$ form, which is discussed in relation to possible reaction intermediates of nitrite reductases.

Experimental Section

Spectral Measurements. Samples for all spectral measurements were prepared under argon atmosphere with minimal exposure to light. Electronic absorption spectral measurements were made on a Hitachi 330 spectrophotometer. Low-temperature absorption spectra were obtained by using a DN1704 variable-temperature liquid nitrogen cryostat equipped with digital temperature controller DTC2 (Oxford Instruments). Proton NMR spectra at 300 MHz and deuterium NMR spectra at 46.1 MHz were recorded with a Nicolet NT-300 spectrometer

(9) Suzuki, S.; Yoshimura, T.; Kohzuma, T.; Shidara, S.; Masuko, M.; Sakurai, T.; Iwasaki, H. *Biochem. Biophys. Res. Commun.* **1989**, *164*, 1366-1372.

(10) Shimada, H.; Orii, Y. *FEBS Lett.* **1975**, *54*, 237-240.

(11) Fujita, E.; Fajer, J. *J. Am. Chem. Soc.* **1983**, *105*, 6743-6745.

(12) Stolzenberg, A. M.; Strauss, S. H.; Holm, R. H. *J. Am. Chem. Soc.* **1981**, *103*, 4763-4778.

(13) (a) Richardson, P. F.; Chang, C. K.; Spaulding, L. D.; Fajer, J. *J. Am. Chem. Soc.* **1979**, *101*, 7736-7739. (b) Richardson, P. F.; Chang, C. K.; Spaulding, L. D.; Fajer, J. *J. Phys. Chem.* **1979**, *83*, 3420-3424. (c) Chang, C. K.; Hanson, L. K.; Richardson, P. F.; Young, R.; Fajer, J. *Proc. Natl. Acad. Sci. U.S.A.* **1981**, *78*, 2652-2656. (d) Fujita, E.; Chang, C. K.; Fajer, J. *J. Am. Chem. Soc.* **1985**, *107*, 7665-7669 and references therein.

(14) Finnegan, M. G.; Lappin, A. G.; Scheidt, W. R. *Inorg. Chem.* **1990**, *29*, 181-185.

(15) Nasri, H.; Wang, Y.; Huynh, B. H.; Scheidt, W. R. *J. Am. Chem. Soc.* **1991**, *113*, 717-719.

(16) Abbreviations: OEC, 7,8-dihydrooctaethylporphyrin dianion (chlorin); OEiBC, mixture of *trans*- and *cis*-2,3,7,8-tetrahydrooctaethylporphyrin dianion (isobacteriochlorin).

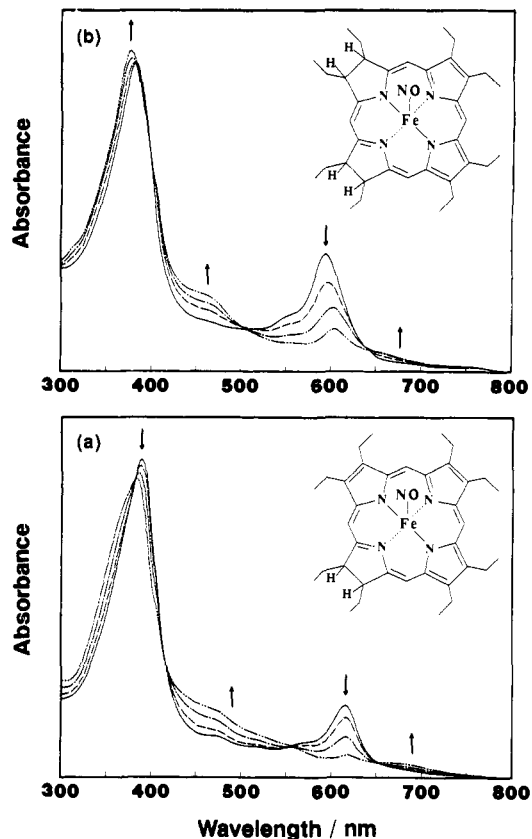


Figure 1. Electronic absorption spectral changes for the titration of (OEC) $\text{Fe}^{\text{II}}\text{NO}$ (0.05 mM) (a) and (OEiBC) $\text{Fe}^{\text{II}}\text{NO}$ (0.06 mM) (b) with silver hexafluoroantimonate in dichloromethane.

equipped with a 1280 computer system. Proton chemical shifts were referenced to Me_4Si internal standard, and downfield shifts are given a positive sign. ESR spectra were obtained on a JEOL PE-2X spectrometer operating at X-band frequencies. FT-IR spectra were recorded on a Nicolet 20 DXB spectrometer, and low-temperature IR spectral measurements were made on a Shimadzu FTIR-4000.

Materials. Dichloromethane and *n*-hexane were refluxed over CaH_2 for 3 h and then distilled. Silver hexafluoroantimonate and tetra-*n*-butylammonium iodide were used as received.

Iron complexes of chlorin and isobacteriochlorin were light and dioxygen sensitive. Consequently, these complexes were prepared and manipulated under an argon atmosphere. Iron(III) octaethylchlorin (OEC) and iron(III) octaethylisobacteriochlorin (OEiBC)¹⁷ complexes were prepared as described.^{12,19,20} (OEC) $\text{Fe}^{\text{II}}\text{NO}$ and (OEiBC) $\text{Fe}^{\text{II}}\text{NO}$ were synthesized by reduction of (OEC) $\text{Fe}^{\text{III}}\text{Cl}$ and (OEiBC) $\text{Fe}^{\text{III}}\text{Cl}$ with 30% $\text{CH}_3\text{SH}/\text{CH}_3\text{OH}$ in dichloromethane, followed by addition of NO. Nitric oxide obtained from Takachiho Trading Co. was passed through a KOH column to remove higher nitrogen oxides. The saturated ring- d_2 and methylene deuterated OEC derivative was prepared with isoamyl alcohol- d_1 which was obtained by deuterium exchange of deuterium oxide.²¹ Deuterium was introduced to the meso positions by using the $\text{D}_2\text{SO}_4\text{-D}_2\text{O}$ method.²² The 15,20-meso- d_2 -OEC complex was synthesized by using a modification of 5,10-meso deuteration.²⁰ The saturated ring- d_4 -15-meso- d_1 -OEiBC complex was prepared with isoamyl alcohol- d_1 .

Oxidation of (OEC) $\text{Fe}^{\text{II}}\text{NO}$. (OEC) $\text{Fe}^{\text{II}}\text{NO}$ (80 mg, 0.13 mmol) was dissolved in 10 mL of dichloromethane, and a dichloromethane solution (1 mL) of silver hexafluoroantimonate (44 mg, 0.13 mmol) as an ox-

(17) All the OEiBC complexes in this study consist of a mixture of two or more diastereomers owing to the presence of two diastereomers (C_2 and C_s symmetries) of H_2OEiBC ^{18,26} (Figure 6).

(18) Angst, C.; Kajiwara, M.; Zass, E.; Eschenmoser, A. *Angew. Chem., Int. Ed. Engl.* **1980**, *19*, 140-141.

(19) Whitlock, H. W.; Hanauer, Jr. R.; Oester, M. Y.; Bower, B. K. *J. Am. Chem. Soc.* **1969**, *91*, 7485-7489.

(20) Fuhrhop, J. H.; Smith, K. M. In *Porphyrins and Metalloporphyrins*; Smith, K. M., Ed.; Elsevier: Amsterdam, 1975; pp 766-769.

(21) Hobden, F. W.; Johnston, E. F.; Weldon, L. H. P.; Wilson, C. L. *J. Chem. Soc.* **1939**, 61-67.

(22) Bonnett, R.; Gale, I. A. D.; Stephenson, G. F. *J. Chem. Soc. C* **1967**, 1168-1172.

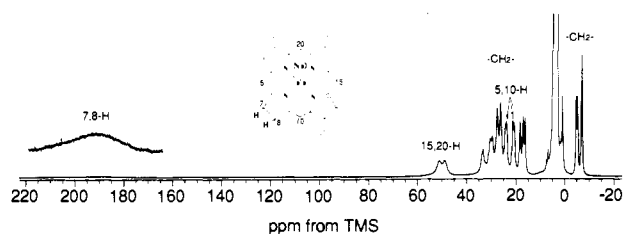


Figure 2. Proton NMR spectrum of the oxidation product of (OEC)- $\text{Fe}^{\text{II}}\text{NO}$ in dichloromethane- d_2 at 22 °C.

dizing reagent was added dropwise to the solution. The initial green solution turned to yellowish brown. The resultant solution was filtered to remove silver. 20 mL of *n*-hexane was slowly added to the filtrate while swirling, and the solution was left at room temperature. Fine black precipitate of the product was obtained by filtration (63 mg, 56%).

Oxidation of (OEiBC) $\text{Fe}^{\text{II}}\text{NO}$. (OEiBC) $\text{Fe}^{\text{II}}\text{NO}$ (22 mg, 0.035 mmol) was dissolved in 5 mL of dichloromethane, and silver hexafluoroantimonate (12 mg, 0.035 mmol) in dichloromethane (1 mL) was added dropwise to the solution. The blue solution turned to green and then greenish yellow. The solution was filtered, 20 mL of *n*-hexane was slowly added to the filtrate, and the solution was kept at room temperature for several hours. The solution was decanted, and a residual solid of the product was dried under vacuum.

Results

Chemical Oxidation. Chemical oxidation of (OEC) $\text{Fe}^{\text{II}}\text{NO}$ and (OEiBC) $\text{Fe}^{\text{II}}\text{NO}$ was performed with silver hexafluoroantimonate (AgSbF_6) in dichloromethane. The oxidation of (OEC) $\text{Fe}^{\text{II}}\text{NO}$ caused a small shift of the Soret band, a loss of the characteristic band for chlorin complexes at 616 nm, and appearance of weak broad bands stretching into the near-infrared region (Figure 1a) characteristic of chlorin π -cation radicals. The oxidation of (OEiBC) $\text{Fe}^{\text{II}}\text{NO}$ led to similar spectral changes (Figure 1b). These spectral alterations were completely reversible upon reduction with one equimolar amount of tetra-*n*-butylammonium iodide (TBAI). These spectral features are identical to the previous results obtained by electrochemical oxidation.¹¹ We also followed the oxidation of (OEC) $\text{Fe}^{\text{II}}\text{NO}$ and (OEiBC) $\text{Fe}^{\text{II}}\text{NO}$ by ESR spectroscopy. Both of the nitrosyl complexes exhibited the three-line ESR spectrum at $g = 2.05$ with $a_N = 17$ G in dichloromethane at room temperature. Upon oxidation, the ESR signals decreased their intensities and finally disappeared when one equimolar amount of AgSbF_6 was added. The ESR spectra of (OEC) $\text{Fe}^{\text{II}}\text{NO}$ and (OEiBC) $\text{Fe}^{\text{II}}\text{NO}$ were also completely recovered by adding (TBAI). Similar spectral alterations were observed at 77 K. The IR spectra of these oxidation products exhibited the NO stretching bands at 1692 and 1712 cm^{-1} , in Nujol, respectively, indicating that NO is bound to the iron of the π -cation radicals with the same bent Fe-NO bonds as for the unoxidized complexes.¹¹ These spectral observations suggest that both of nitrosyl complexes are chemically oxidized to their π -cation radicals.

Characterization of the Oxidation Products. More unambiguous evidence for the formation of (OEC) $\text{Fe}^{\text{II}}\text{NO}$ and (OEiBC) $\text{Fe}^{\text{II}}\text{NO}$ π -cation radicals was obtained by proton and deuterium paramagnetic NMR. The proton NMR spectrum of the oxidation product of (OEC) $\text{Fe}^{\text{II}}\text{NO}$ exhibited well-resolved hyperfine-shifted proton NMR resonances (Figure 2). Signal assignments were made by using selectively deuterated derivatives, as demonstrated in Figure 3. Upon oxidation, the methylene deuterium resonances for the pyrrole rings are observed in a downfield region (Figure 3a). A multiple splitting of the methylene deuterium resonances (+16 to +33 and -4.4 to -6.5 ppm) implies that NO bound to iron makes two methylene deuteriums nonequivalent. Meso deuterium resonances exhibit oxidation-induced downfield shift as illustrated in Figure 3b,c. An NMR signal for the saturated pyrrole ring deuteriums (7,8-positions) is observed in the far-downfield region at 184 ppm, as shown in Figure 3a. Such a large shift for the saturated pyrrole ring deuteriums is hardly due to metal oxidation, but rather result from the chlorin π -cation radical in which a substantial amount of positive π -spin density on the α -carbons of the saturated pyrrole ring is delocalized onto C_βH

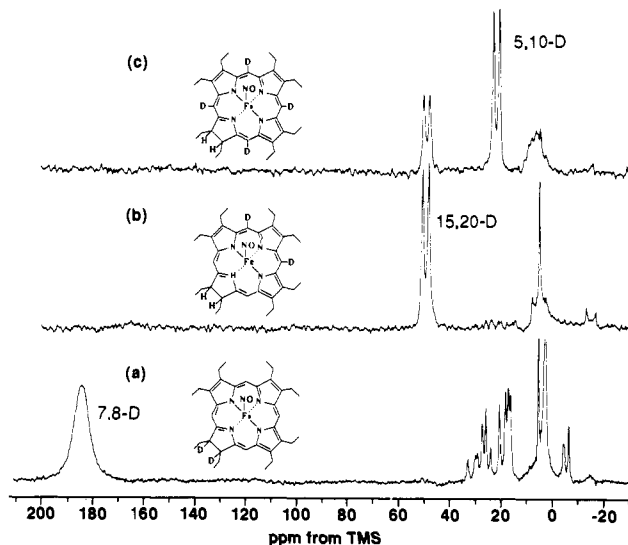


Figure 3. Deuterium NMR spectra of selectively deuterated (OEC)- $\text{Fe}^{\text{II}}\text{NO}$ π -cation radicals in dichloromethane at 22 °C: (a) saturated pyrrole ring- d_2 and methylene deuterated, (b) 5,10-meso- d_2 , and (c) meso- d_4 complexes.

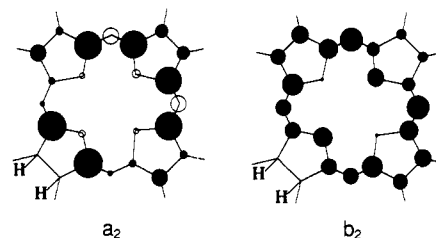


Figure 4. Electron spin distribution of chlorin π -cation radicals (a_2 and b_2) by SCF Pariser-Parr-Pople MO calculations from ref 24. Filled and open circles correspond to positive and negative spin densities, respectively.

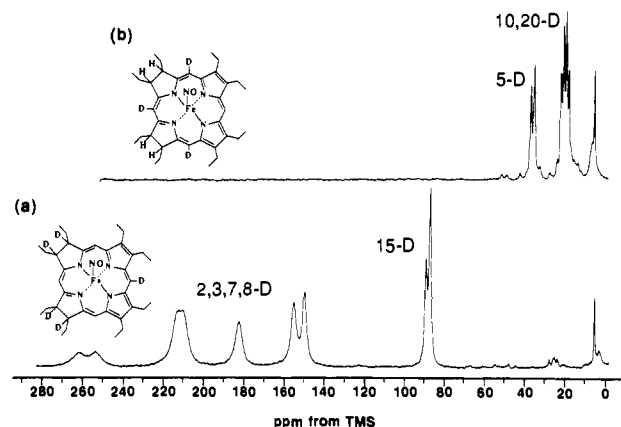


Figure 5. Deuterium NMR spectra of selectively deuterated (OEiBC)- $\text{Fe}^{\text{II}}\text{NO}$ π -cation radicals in dichloromethane at 22 °C: (a) saturated pyrrole ring- d_4 -15-meso- d_1 and (b) 5,10,20-meso- d_3 complexes.

via hyperconjugation.^{23a} According to MO calculations,^{24,25} two nearly degenerated ground states (2A_2 and 2B_2), separated by ~ 2000 cm^{-1} , are possible for oxidized chlorins. The a_2 radical orbital bears a large spin density at the α -carbons of the saturated pyrrole ring, whereas the b_2 radical has spin density at meso carbons and pyrrole nitrogens (Figure 4). The large downfield

(23) (a) Jesson, J. P. In *NMR of Paramagnetic Molecules*; La Mar, G. N., Horrocks, W. D., Holm, R. H., Eds.; Academic Press: New York, 1973; pp 1-52. (b) Kreilick, R. W. *Ibid.* pp 595-626.

(24) Fajer, J.; Davis, M. S. In *The Porphyrins*; Dolphin, D., Ed.; Academic Press: New York, 1979; Vol. 4, pp 197-256.

(25) Hanson, L. K.; Chang, C. K.; Davis, M. S.; Fajer, J. *J. Am. Chem. Soc.* **1981**, *103*, 663-670.

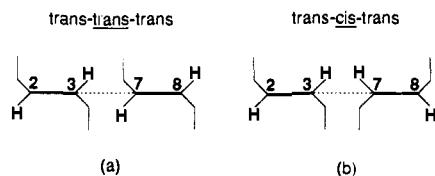


Figure 6. Two diastereomers for H_2OEiBC : *ttt* (a), *tct* (b). Only the saturated pyrrole rings (2,3,7,8-positions) are represented.

Table I. Deuterium NMR Chemical Shift Values (δ_{obs}) for (OEC)Fe^{II}NO and (OEiBC)Fe^{II}NO π -Cation Radicals^a

	(OEC)Fe ^{II} NO(SbF ₆)
-CH ₂ -	-6.5 ^b , -4.8 ^b , -4.4 ^b , 16, 17, 18 20, 24, 26, 27, 29, 30, 33
15,20-meso	49, 51
5,10-meso	22, 24
saturated ring	184
	(OEiBC)Fe ^{II} NO(SbF ₆)
15-meso	87, 89
10,20-meso	18, 20, 21, 22
5-meso	35, 37
saturated rings	150, 155, 182 210, ^c 212, ^c 254, 262

^a 5–10 mM in CH_2Cl_2 at 22 °C, chemical shifts referenced to TMS and in ppm. ^b The methylene deuterium resonances of the saturated pyrrole ring. ^c These resonances are not resolved below 0 °C.

shift (184 ppm) for the 7,8-deuteriums of the (OEC)Fe^{II}NO π -cation radical is translated into large π spin density on the pyrrole α -carbons and is reasonably attributed to the a_2 radical state.

The proton NMR spectrum of the oxidation product of (OEiBC)Fe^{II}NO was much more complicated. As seen in Figure 5, however, an identification of the oxidation product was accomplished by using selectively deuterated samples. 5,10,20-Meso deuterium resonances exhibit oxidation-induced downfield shift, comprised of two sets of six signals (Figure 5b). Apparently, 10,20- and 5-meso deuteriums have a different environment, so that the most downfield signals are assigned to the 5-meso deuterium and the 18–22 ppm signals are to the 10,20-meso deuteriums, respectively. 15-Meso deuterium resonances exhibit larger downfield shifts at 87 and 89 ppm (Figure 5a). Each of these meso deuterium resonances is split into a doublet. Since H_2OEiBC contains two diastereomers²⁶ (Figure 6) having C_2 and C_s symmetry, metalated five-coordinate or mixed liganded six-coordinate OEiBC complexes bear three diastereomers.^{12,27} However, the splitting of the meso deuterium resonances into a doublet indicates that the oxidation product of (OEiBC)Fe^{II}NO has only two diastereomers. As illustrated in Figure 5a, deuterium NMR signals for the saturated pyrrole ring deuteriums (2,3,7,8-positions) appear in the far downfield region (+150 to +260 ppm). The unusually large downfield shift for the 2,3,7,8-deuterium resonances should be attributed to a radical spin on the isobacteriochlorin ring, rather than to the iron-centered paramagnetic effect. Moreover, the large downfield shift for the saturated ring deuterium resonances is rationalized by an a_2 (for an idealized C_{2v} symmetry) radical state. A multiple splitting of the 2,3,7,8-deuterium resonances is consistent with the presence of two diastereomers and with different spin densities predicted for inboard (3,7-position) and outboard (2,8-position) α -carbons of the saturated rings,¹³ but the assignment of each signal has not yet been made. Some of the signal assignments are summarized in Table I.

Variable-Temperature Measurements. Variable-temperature deuterium NMR measurements were examined in the range from 193 to 298 K for (OEC)Fe^{II}NO and (OEiBC)Fe^{II}NO π -cation radicals. Temperature dependence of the deuterium NMR signals is depicted as Curie law plots in Figure 7, in which deviation from

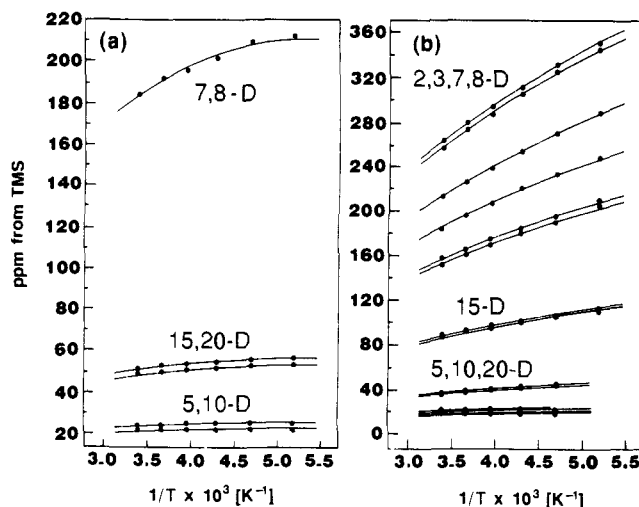


Figure 7. Temperature dependence of the saturated pyrrole ring and meso deuterium signals of the (OEC)Fe^{II}NO π -cation radical (a) and the (OEiBC)Fe^{II}NO π -cation radical (b). The chemical shifts are plotted against $1/T$ (Curie law plot). Solid lines (b) represent the simulation results.

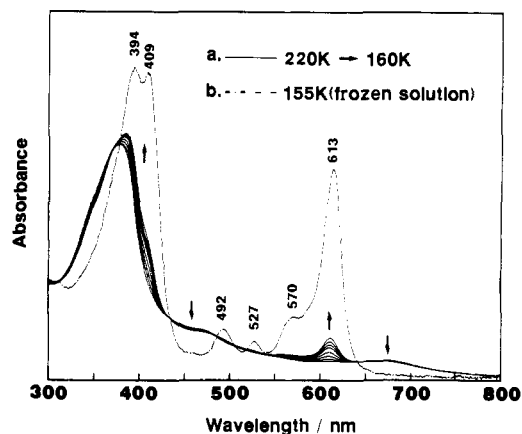


Figure 8. Electronic absorption spectra of the (OEC)Fe^{II}NO π -cation radical in the 220–160 K range in CH_2Cl_2 (a) and in CH_2Cl_2 frozen solution at 155 K (b). Temperature decreases as indicated by arrows.

linearity and the far-downfield shift intercept at high temperature is seen for the saturated ring and meso deuterium resonances. When the temperature was lowered, all the signals shifted with more upfield shift bias than expected for the Curie law features. The unusual temperature dependence implies that (OEC)Fe^{II}NO and (OEiBC)Fe^{II}NO π -cation radicals are in a thermal admixture of two different states.^{28b,c}

To gain further insight into this temperature-dependent behavior, the electronic absorption spectra of (OEC)Fe^{II}NO and (OEiBC)Fe^{II}NO π -cation radicals were studied at various temperatures between 220 and 80 K in dichloromethane. As demonstrated in Figure 8, when the temperature was lowered to 160 K of the (OEC)Fe^{II}NO π -cation radical solution, the band at around 615 nm appeared and the Soret band was red shifted with several isobestic points (Figure 8a, solid lines). When the dichloromethane solution was further cooled to a frozen temperature at 155 K, a large spectral change was observed, i.e., appearance of an intense absorption peak at 613 nm and split Soret band at 394 and 409 nm to yield an entirely new spectrum (Figure 8b), which was almost identical with the one for the ligand-bound complex (vide infra). These spectral changes were fully reversible

(26) Stolzenberg, A. M.; Spreer, L. O.; Holm, R. H. *J. Am. Chem. Soc.* **1980**, *102*, 364–370.

(27) Sullivan, Jr. E. P.; Grantham, J. D.; Thomas, C. S.; Strauss, S. H. *J. Am. Chem. Soc.* **1991**, *113*, 5264–5270.

(28) (a) Morishima, I.; Shiro, Y.; Takamuki, Y. *J. Am. Chem. Soc.* **1983**, *105*, 6168–6170. (b) Morishima, I.; Takamuki, Y.; Shiro, Y. *J. Am. Chem. Soc.* **1984**, *106*, 7666–7672. (c) Morishima, I.; Fujii, H.; Shiro, Y.; Sano, S. *J. Am. Chem. Soc.* **1986**, *108*, 3858–3860.

(29) Davis, M. S.; Forman, A.; Fajer, J. *Proc. Natl. Acad. Sci. U.S.A.* **1979**, *76*, 4170–4174.

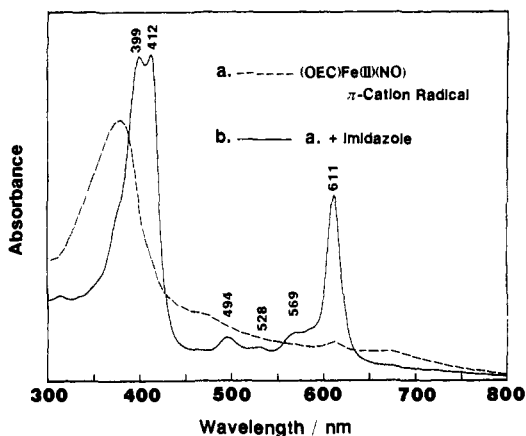


Figure 9. Electronic absorption spectra of (OEC)Fe^{II}NO π -cation radical in the absence of imidazole (a) and in the presence of an excess amount of imidazole (b) in CH₂Cl₂ at 220 K.

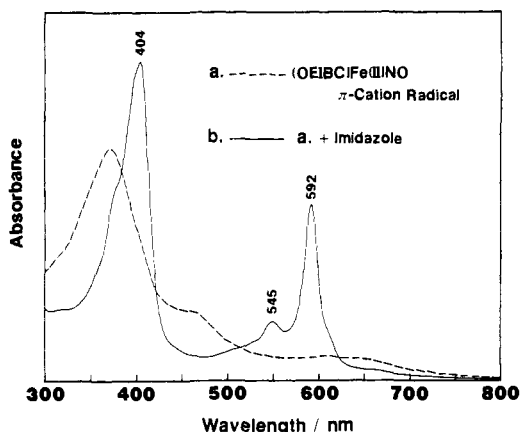


Figure 10. Electronic absorption spectra of (OEiBC)Fe^{II}NO π -cation radical in the absence of imidazole (a) and in the presence of an excess amount of imidazole (b) in CH₂Cl₂ at 220 K.

with raising or lowering temperature, showing that NO is still bound to iron during temperature variation. It is therefore likely that the dramatic spectral changes at 155–160 K result from ligand (SbF₆⁻) binding in the frozen solution. In contrast, the electronic absorption spectrum of the (OEiBC)Fe^{II}NO π -cation radical remained unchanged when the temperature was lowered to 80 K.

Ligand Effects on the π -Cation Radicals. In order to further examine the effect of axial ligation on the electronic structure of the π -cation radical of (OEC)Fe^{II}NO, imidazole was added at 220 K to an (OEC)Fe^{II}NO π -cation radical solution. The addition of an excess amount of imidazole to the π -radical solution afforded a new spectrum (Figure 9) similar to that of the frozen sample of the (OEC)Fe^{II}NO π -cation radical. Moreover, when the temperature was raised to 300 K, the spectrum of the imidazole adduct changed to that of a bis(imidazole) complex, [(OEC)Fe^{III}(Im)₂]⁺, having characteristic absorption maxima at 403 and 583 nm. This finding suggests that the (OEC)Fe^{II}NO π -cation radical is not reduced to (OEC)Fe^{II}NO at room temperature, but rather NO is readily replaced by imidazole. Addition of other ligands such as pyridine, THF, and acetonitrile resulted in similar spectral changes.

The addition of an excess amount of imidazole to the (OEiBC)Fe^{II}NO π -cation radical solution at 220 K gave a new band at 592 nm and the Soret band at 404 nm (Figure 10), indicating substantial changes in the electronic structure. This imidazole adduct was also changed to [(OEiBC)Fe^{III}(Im)₂]⁺ when the temperature was raised to 300 K. The absorption spectral data are compiled in Table II.

Discussion

Electronic Structures of Iron(II) Nitrosyl π -Cation Radicals. It was demonstrated here that iron(II) nitrosyl π -cation radicals

Table II. Electronic Absorption Spectral Characteristics of the Chlorin and Isobacteriochlorin Complexes^a

L, L'	λ_{\max}/nm (relative intensity)
(OEC)Fe ^{II} (L)(L')	
NO ⁺ , SbF ₆ ^{-b}	394 (1.000), 409 (0.981), 492 (0.0617), 527 (0.0202), 570 (0.0108), 613 (0.636)
NO ⁺ , Im ^c	399 (1.000), 412 (1.007), 494 (0.131), 528 (0.103), 569 (0.147), 611 (0.570)
NO ⁺ , Py ^c	398 (1.000), 411 (0.922), 496 (0.0957), 530 (0.0738), 571 sh (0.127), 613 (0.509)
NO ⁺ , CH ₃ CN ^d	396 (1.000), 409 (0.919), 493 (0.103), 530 (0.0765), 567 (sh) (0.110), 612 (0.454)
NO ⁺ , THF ^c	391 (1.000), 407 (0.771), 493 (0.0809), 526 (0.0700), 570 (0.0938), 613 (0.378)
CO, N-MeIm ^c	399 sh (1.000), 409 (1.174), 492 (0.0884), 566 sh (0.0988), 608 (0.406)
(OEiBC)Fe ^{II} (L)(L')	
NO ⁺ , Im ^c	404 (1.000), 545 (0.184), 592 (0.549)
CO, N-MeIm ^c	396 (1.000), 545 (0.179), 589 (0.556)

^a 0.03–0.05 mM in CH₂Cl₂. ^b In CH₂Cl₂ frozen solution at 155 K. ^c At 220 K. ^d At 230 K. ^e Reference 12 in benzene.

of the chlorin and isobacteriochlorin complexes are successfully formed by the chemical oxidation of (OEC)Fe^{II}NO and (OEiBC)Fe^{II}NO without oxidation of the saturated pyrrole ring. These π -cation radicals were ESR silent, and hence the ESR spectra did not serve as a diagnosis of the electronic structure determination of the π -radical complexes. Enhanced electron spin relaxations for the (OEC)Fe^{II}NO and (OEiBC)Fe^{II}NO π -radical complexes are fortunate for the paramagnetic NMR, as visualized in the well-defined NMR spectra (Figures 2, 3, and 5). An isotropic NMR hyperfine shift for the π -radical system is related through eqs 1–3 to the π -electron spin density at the meso carbons

$$\left(\frac{\Delta H}{H}\right)_{\text{iso}} = A^H \frac{\gamma_e}{\gamma_H} \frac{g\beta S(S+1)}{3kT} \quad (1)$$

$$A^H = Q\rho_C \quad (2)$$

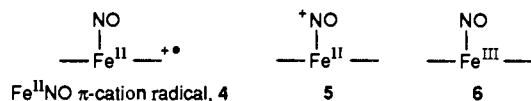
$$A^H = (B_0 + B_2 \cos^2 \theta)\rho_{C-\text{CH}} \quad (3)$$

(ρ_C , eq 2) and the α -carbons of the saturated pyrrole ring ($\rho_{C-\text{CH}}$, eq 3). Here, eq 1 relates the observed isotropic shift ($\Delta H/H$)_{iso} with the proton hyperfine coupling constant (A^H).²³ Equations 2 and 3 are the McConnell relations which connect A^H with the π -spin density on the meso carbons and the α -carbons of the saturated pyrrole ring, respectively. B_0 and B_2 are constants, and θ is the dihedral angle between the 2p_z orbital of the α -carbon and the plane defined by the α - and β -carbons and the proton.²⁴ With these equations, the observed hyperfine shifts of the meso and saturated ring deuteriums are readily translated into π -spin densities at the meso and α -carbons, respectively.

In chlorins,²⁴ θ ranges between 30° and 45°; therefore, a large downfield shift (184 ppm) for the saturated pyrrole ring deuteriums of the (OEC)Fe^{II}NO π -cation radical is translated to large π -spin density of $\rho = 0.039$ – 0.063 on the α -carbons of the saturated ring and is consistent with the a₂ radical state. In the a₂ radical state, negative spin densities are expected at the meso 15,20-positions.^{24,25} In fact, downfield contact shifts (49, 51 ppm) for the meso deuteriums which correspond to the negative π -spin density ($\rho = -0.030$) on the meso carbons are induced for the (OEC)Fe^{II}NO π -cation radical. Large downfield shifts (+150 to +262 ppm) for the saturated pyrrole ring deuteriums of the (OEiBC)Fe^{II}NO π -cation radical correspond to large π -spin densities of $\rho = 0.032$ – 0.052 to 0.056 – 0.090 on the α -carbons of the saturated rings, which is in agreement with the a₂ radical state. These results obtained by NMR spectroscopy are consistent with ESR and theoretical results reported before,^{13,24,25} and the nitrosyl iron(II) chlorin and isobacteriochlorin π -cation radicals belong to general classes of hydroporphyrins that have been shown to conform a₂ profiles.

The temperature dependences of the NMR signals for the π -cation radicals of (OEC)Fe^{II}NO and (OEiBC)Fe^{II}NO showed

slight deviations from normal Curie law behavior (Figure 6), which could be explained in terms of a thermal admixture of two different states.^{28b,c} This unusual feature was ascertained by variable-temperature absorption spectral measurements. For the (OEC)Fe^{II}NO π -cation radical, lowering the temperature to 160 K and freezing the π -radical solution caused reversible absorption spectral changes indicative of substantial changes in the electronic structure, as manifested by a new characteristic absorption peak at 613 nm at low temperatures (Figure 8). This reminds us of the previous finding by Dolphin et al.³⁰ that upon freezing of a dichloromethane solution of a Ni^{II}TPP π -cation radical to 77 K, an internal electron transfer affords the corresponding nickel(III) porphyrin. At room temperature the nickel(II) porphyrin π -cation radical solution exhibited a single ESR signal at $g = 2.0041$ with a peak-to-peak separation of 47.2 G, while at 77 K the π -radical solution showed the signals with $g_{\perp} = 2.286$ and $g_{\parallel} = 2.086$, consistent with a low-spin d^7 (Ni(III)) electronic configuration. This valence isomerization from the Ni(II) π -cation radical to the Ni(III) complex possibly results from ligation of an anion such as PF₆⁻ or ClO₄⁻ at low temperature. Further, Salehi et al.³¹ showed that the axial ligation (water or methanol) converts the cobalt(II) porphyrin π -cation radical to a cobalt(III) porphyrin complex. Since the (OEC)Fe^{II}NO π -cation radical is ESR silent at 77 K, the absorption spectral changes of the π -radical solution upon freezing of the solution are indicative of valence isomerization from the chlorin π -cation radical **4** to Fe^{II}NO⁺ (**5**) or Fe^{III}NO (**6**) chlorin complex, which is in a diamagnetic state.



Wayland and Olson have reported³² that a nitric oxide adduct of (TPP)Fe^{III}Cl is formulated as (TPP)Fe^{II}(NO⁺)(Cl), on the basis of its absorption spectrum characteristic of a ferrous low-spin complex such as (TPP)Fe^{II}(Py)₂. Accordingly, the valence isomers, **5** and **6**, could be distinguished by their absorption spectra. In fact, the absorption spectrum (λ_{max} 394, 409, 492, 527, 570, 613) of the frozen sample of the (OEC)Fe^{II}NO π -cation radical solution is similar to that of (OEC)Fe^{II}(CO)(N-MeIm) (λ_{max} 399sh, 409, 492, 566sh, 608)¹² but different from those of Fe(III) low-spin chlorin complexes. It is thus likely that the (OEC)Fe^{II}NO π -cation radical is formulated as (OEC)Fe^{II}(NO⁺)(SbF₆⁻) at low temperature due to ligation of SbF₆⁻. The absorption spectrum of the imidazole adduct of the (OEC)Fe^{II}NO π -cation radical (λ_{max} 399, 412, 494, 528, 569, 611) is also similar to that of the frozen sample of the radical, indicating the imidazole adduct to be (OEC)Fe^{II}(NO⁺)(Im). Further, the addition of other ligands, L (L = pyridine, THF, acetonitrile) afforded similar absorption spectra (Table II), suggesting the formation of (OEC)Fe^{II}(NO⁺)(L) complexes. The electrochemical oxidation of (OEC)Fe^{II}NO reported in ref 11 was done in butyronitrile and yielded a π -cation radical complex at room temperature. This different feature between acetonitrile and butyronitrile is surprising, and the reason for this is not established yet.

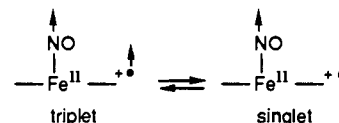
While the absorption spectrum of the (OEiBC)Fe^{II}NO π -radical solution did not show any appreciable changes even at 80 K, the addition of an excess amount of imidazole led to large spectral changes to give a entirely new spectrum (λ_{max} 404, 545, 592) which closely resembles that of (OEiBC)Fe^{II}(CO)(N-MeIm) (λ_{max} 396, 545, 589),¹² suggesting the formation of (OEiBC)Fe^{II}(NO⁺)(Im). It is therefore concluded that the axial ligation of imidazole to chlorin and isobacteriochlorin π -cation radicals **4** produces Fe^{II}NO⁺ complex **5**.³³ Recently, Sullivan and Strauss³⁴ have also

demonstrated that a five-coordinate iron(III) isobacteriochlorin complex binds CO at its sixth coordination site by simultaneous oxidation of the macrocycle to a π -cation radical and reduction of iron(III) to iron(II).

The valence isomerization (**4** \rightarrow **5**) could be determined by the relative energies of the metal d and the macrocycle π -radical orbitals. If the metal d-orbital energy level (in this case Fe(d_{z^2})-NO(σ_N) hybrid orbital) is preferentially raised up by axial ligation, the valence isomerization may be facilitated. Thus, the Fe-NO hybrid orbital could move to much higher energy level by ligation of a strong ligand (imidazole), leading **5** to be favorable for both (OEC)Fe^{II}NO and (OEiBC)Fe^{II}NO π -cation radicals. Since the macrocycle π -orbital levels of isobacteriochlorin complexes are higher than those of chlorin complexes,^{11,13} the SbF₆⁻ ligand is not strong enough to raise the Fe-NO hybrid orbital energy higher than isobacteriochlorin macrocycle π -orbital energy.

In the Fe^{II}NO complexes **4**, the odd electron on nitric oxide occupies a molecular orbital of nitric oxide σ_N and Fe d_{z^2} character,³⁵ resulting in essentially a one-electron Fe-NO covalent σ bond.^{32b} On the other hand, the d_{z^2} and NO π^* orbitals of **5** are empty, so that the Fe^{II}NO⁺ fragment has no covalent σ -bond character and this instability can be partially compensated by d_{π} - p_{π} back-bonding due to linear Fe-NO bonding.^{32b} Thus, NO⁺ bound to (OEC)Fe^{II}(NO⁺)(Im) and (OEiBC)Fe^{II}(NO⁺)(Im) is expected to be more labile than NO in (OEC)Fe^{II}NO and (OEiBC)Fe^{II}NO π -cation radicals.¹¹ In fact, **5** was readily converted to the bis(imidazole) complex at room temperature.

Intramolecular Magnetic Coupling of (OEiBC)Fe^{II}NO π -Cation Radical. Inspection of Figure 6b shows that the hyperfine-shifted NMR signals for (OEiBC)Fe^{II}NO π -cation radical exhibit a slight deviation from normal Curie law behavior. While this observation would be explained by formation of its dimer which could induce more upfield shift bias than expected on the basis of the Curie law when the temperature is lowered, the frozen sample of the π -cation radicals did not show any absorption at around 900 nm characteristic of π - π dimer formation.³⁶ Further, this unusual feature is not attributed to valence isomerization between **4** and **5**, as confirmed by variable-temperature absorption spectral measurements, but rather possibly due to a thermal admixture of ferromagnetic (triplet) and antiferromagnetic (singlet) states,³⁷ as described below.



Previously, Reed et al.³⁸ showed that a metalloporphyrin π -cation radical such as (TPP)Fe^{III}(ClO₄)₂ exhibits intramolecular ferromagnetic coupling when their magnetic orbitals are orthogonal due to an in-plane structure. On the other hand, metalloporphyrin π -cation radicals such as (TPP)Fe^{III}Cl(SbCl₆) with a saddle-shaped structure experience antiferromagnetic coupling, because overlap between the metal and porphyrin orbitals is symmetry allowed.³⁸ a_2 symmetry of the (OEiBC)Fe^{II}NO π -

(33) These findings could be established more firmly, particularly by IR measurements at low temperature, since the NO⁺ in the Fe^{II}(NO⁺) complexes is linear and the NO⁺ stretch should be observed around 1800 cm⁻¹. Because of the difficulty of such experiments, we did not do this at this moment.

(34) Sullivan, Jr. E. P.; Strauss, S. H. *Inorg. Chem.* **1989**, *28*, 3093-3095.
 (35) (a) Kon, H.; Kataoka, N. *Biochemistry* **1969**, *8*, 4757-4762. (b) Osterhuris, W. T.; Lang, G. *J. Chem. Phys.* **1969**, *50*, 4381-4387. (c) Yonetani, T.; Yamamoto, H.; Erman, J. E.; Leigh, Jr. J. S.; Reed, G. H. *J. Biol. Chem.* **1972**, *247*, 2447-2455. (d) Yoshimura, T. *Bull. Chem. Soc. Jpn.* **1978**, *51*, 1237-1238. (e) Yoshimura, T. *Inorg. Chem.* **1986**, *25*, 688-691.

(36) (a) Fuhrhop, J. H.; Wasser, P.; Riesner, D.; Mauzerall, D. *J. Am. Chem. Soc.* **1972**, *94*, 7996-8001. (b) Mengersen, C.; Subramanian, J.; Fuhrhop, J. H. *Mol. Phys.* **1976**, *32*, 893-897. (c) Song, H.; Orosz, R. D.; Reed, C. A.; Scheidt, W. R. *Inorg. Chem.* **1990**, *29*, 4274-4282 and references therein.

(37) Fujii, H. and Morishima, I. Submitted for publication.
 (38) (a) Gans, P.; Buisson, G.; Duèe, E.; Marchon, J.-C.; Erlar, B. S.; Scholz, W. F.; Reed, C. A. *J. Am. Chem. Soc.* **1986**, *108*, 1223-1234. (b) Erlar, B. S.; Scholz, W. F.; Lee, Y. J.; Scheidt, W. R.; Reed, C. A. *J. Am. Chem. Soc.* **1987**, *109*, 2644-2652.

(30) (a) Dolphin, D.; Niemi, T.; Felton, R. H.; Fujita, I. *J. Am. Chem. Soc.* **1975**, *97*, 5288-5290. (b) Johnson, E. C.; Niemi, T.; Dolphin, D. *Can. J. Chem.* **1978**, *56*, 1381-1388.

(31) Salehi, A.; Oertling, W. A.; Babcock, G. T.; Chang, C. K. *J. Am. Chem. Soc.* **1986**, *108*, 5630-5631.

(32) (a) Wayland, B. B.; Olson, L. W. *J. C. S. Chem. Commun.* **1973**, 897-898. (b) Wayland, B. B.; Olson, L. W. *J. Am. Chem. Soc.* **1974**, *96*, 6037-6041.

cation radical due to macrocycle reduction allows the π -radical orbital to interact with the iron d orbital, resulting in antiferromagnetic coupling. In this case, the magnetic coupling constant is expected to be small, because the a_2 radical orbital does not have large spin densities at pyrrole nitrogens.^{13,24,25} Suppose that the triplet state of the (OEiBC)Fe^{II}NO π -cation radical possesses slightly higher energy than the singlet state due to moderate spin coupling. The triplet state can be thermally admixed to the singlet state at room temperature. It is therefore likely that NMR hyperfine shifts are represented as a fractional weighted average of the limiting shifts of two extreme states. Then, a simulation of the Curie law plot for the (OEiBC)Fe^{II}NO π -cation radical was performed by taking into account the magnetic interaction given by the Hamiltonian $\mathcal{H} = -JS_1 \cdot S_2$, where S_1 and S_2 are spin vectors for the NO and π -radical spins.³⁹ As shown in Figure 6b, the coupling constant of $J = -46 \text{ cm}^{-1}$ fits well with the experimental values, and a content proportion of the triplet state at 296 K was estimated to be 35%. These results demonstrate that the NO and π -radical spins are weakly antiferromagnetically coupled and this thermal admixture is nearly saturated at room temperature.

Biological Implications. The sixth ligand of heme d_1 in a dissimilatory nitrite reductase has been shown to be nitrogenous ligand (probably the imidazole group of a histidyl residue) by ESR spectra of a NO-bound heme d_1 , which has a superhyperfine

(39) The simulation of the Curie law plot for (OEiBC)Fe^{II}NO π -cation radical was performed with the following equation, $\delta_{\text{obs}} = [\delta'_{s=0}/T + 3(\delta'_{s=1}/T) \exp(-J/kT)] / (1 + 3 \exp(-J/kT)) + \delta_{\text{dia}}$, where $\delta'_{s=0}/T$ and $\delta'_{s=1}/T$, with opposite signs, are the limiting shifts for the singlet and triplet states, respectively, J is an energy separation gap of the singlet and triplet states, and δ_{dia} is a diamagnetic correction based on the NMR shifts for the free base, H₂OEiBC.

structure due to an additional nitrogen atom.⁶ On the other hand, the axial ligand for the siroheme in assimilatory nitrite reductases remains undetermined.⁴⁰ According to the results reported here, the axial ligation, if any, in assimilatory nitrite reductases may prefer the Fe^{II}(NO⁺)(L) complex (5) instead of the π -cation radical (4) as a reaction intermediate during the reduction of nitrite to nitric oxide, and 5 will readily release NO. As noted previously,¹¹ however, the subsequent reaction of nitric oxide to ammonia may require the Fe^{II}NO π -cation radical (4) because of its stability.

In summary, (OEC)Fe^{II}NO and (OEiBC)Fe^{II}NO π -cation radicals were successfully prepared by chemical oxidation and their hyperfine-shifted NMR spectra have demonstrated that the radical orbitals for both π -cation radicals are of an a_2 type. Addition of imidazole to the π -radical solutions promoted valence isomerization to yield (OEC)Fe^{II}(NO⁺)(Im) and (OEiBC)Fe^{II}(NO⁺)(Im). The model studies reported here certainly raised the possibility that the axial ligation may control the structures of the reaction intermediates and the reactivity of NO bound to iron in nitrite reductases.

To gain further insight into the magnetic interaction between the NO and π -radical spins, detailed studies of solid-state magnetic susceptibilities of the π -cation radicals are under investigation.

Acknowledgment. We thank Dr. T. Yoshimura for helpful discussions concerning syntheses of nitrosyl complexes and Dr. A. Yabe and Mr. T. Ohana for low-temperature IR measurements. We also thank Mr. Y. Ohta for some spectral measurements and Dr. Y. Watanabe and the reviewers for helpful comments.

(40) ESR spectra of spinach nitrite reductase-NO complexes have been observed.^{7,8}

Enantioselective Binding of Tryptophan by α -Cyclodextrin

Kenny B. Lipkowitz,* Srinivasrao Raghobama, and Jia-an Yang

Contribution from the Department of Chemistry, Indiana University-Purdue University at Indianapolis, 1125 East 38th Street, Indianapolis, Indiana 46205. Received July 1, 1991

Abstract: ¹H and ¹³C NMR studies of racemic and optically pure tryptophan binding with α -cyclodextrin are carried out to explain chiral recognition in this guest-host system. The changes in chemical shifts, coupling constants, and relaxation times for the *R* enantiomer are larger than for *S* upon binding, and differential changes of *R* vs *S* in the bound state are larger for the more tightly bound *R* enantiomer. An intermolecular NOE between guest and host places the indole ring near the secondary hydroxyl rim of the cyclodextrin for both enantiomers, suggesting similar modes of binding. Results extracted from molecular dynamics simulations are that both guests are highly localized on the interior of the host, the ammonium group of the zwitterionic tryptophan does not contribute to the recognition process, and the more tightly bound *R* enantiomer forms twice as many hydrogen bonds as its optical antipode, most of which are multiple-contact hydrogen bonds. Both *R* and *S* guests are found to use the same kinds of intermolecular interactions but to a greater or lesser extent. Armstrong's chiral recognition model has been slightly modified but generally remains intact.

Introduction

The intermolecular forces have been exhaustively studied and are thoroughly documented.¹ The way these forces act to form inclusion complexes is now the focus on ongoing studies in molecular recognition.² Less well understood but critical to many disciplines of science is chiral recognition. What are the origins of enantioselectivity? How does a chiral receptor, either natural or synthetic, discriminate between two nonsuperimposable mirror

images that otherwise have identical molecular descriptors? Precisely how intermolecular forces act, in concert, to discriminate between enantiomers is not well established.

In this paper we examine the enantioselective binding of D,L-tryptophan to α -cyclodextrin (CD). We select tryptophan because it is size consistent with α -cyclodextrin and should form inclusion complexes³ and it provides a starting point for future studies of how chiral recognition is enhanced or diminished by replacing the

(1) A well written introductory textbook exists: Rigby, M.; Smith, E. B.; Wakeham, W. A.; Maitland, G. C. *The Forces Between Molecules*; Oxford Science Publications, Clarendon Press: Oxford, 1986.

(2) (a) Cram, D. J. *Angew. Chem., Int. Ed. Engl.* **1988**, *27* (8), 1009. (b) Lehn, J.-M. *Ibid.* **1988**, *27* (8), 89. (c) Rebek, Jr., J. *Ibid.* **1990**, *29* (3), 245.

(3) (a) Bender, M. L.; Komiyama, M. *Cyclodextrin Chemistry*; Springer: New York, 1978. (b) Saenger, W. *Angew. Chem., Int. Ed. Engl.* **1980**, *19*, 344. (c) Szejtli, J. *Cyclodextrins and Their Inclusion Complexes*; Akademiai Kiado: Budapest, 1982. (d) Szejtli, J. *Cyclodextrin Technology*, Kluwer Academic Publishers: Dordrecht, 1988.